Biochimica et Biophysica Acta 1838 (2014) 2838–2851

Contents lists available at ScienceDirect

Biochimica et Biophysica Acta

journal homepage: www.elsevier.com/locate/bbamem

The pore-lining regions in cytochrome c oxidases: A computational analysis of caveolin, cholesterol and transmembrane helix contributions to proton movement

Gene A. Morrill *, Adele B. Kostellow, Raj K. Gupta

Department of Physiology and Biophysics, Albert Einstein College of Medicine, 1300 Morris Park Avenue, Bronx, NY 10461 USA

ARTICLE INFO

Article history:
Received 8 April 2014
Received in revised form 19 June 2014
Accepted 8 July 2014
Available online 15 July 2014

Keywords:
Cytochrome c oxidase
COX-1
Cholesterol
Caveolin
Protein topology
Channels

ABSTRACT

Cytochrome c oxidase (CcO) is the terminal enzyme in the electron transfer chain. CcO catalyzes a four electron reduction of O_2 to water at a catalytic site formed by high-spin heme (a_3) and copper atoms (Cu_B). While it is recognized that proton movement is coupled to oxygen reduction, the proton channel(s) have not been well defined. Using computational methods developed to study protein topology, membrane channels and 3D packing arrangements within transmembrane (TM) helix arrays, we find that subunit-1 (COX-1), subunit-2 (COX-2) and subunit-3 (COX-3) contribute 139, 46 and 25 residues, respectively, to channel formation between the mitochondrial matrix and intermembrane space. Nine of 12 TM helices in COX-1, both helices in COX-2 and 5 of the 6 TM helices in COX-3 are pore-lining regions (possible channel formers). Heme a_3 and the Cu_B sites (as well as the Cu_A center of COX-2) are located within the channel that includes TM-6, TM-7, TM-10 and TM-11 of COX-1 and are associated with multiple cholesterol and caveolin-binding (CB) motifs. Sequence analysis identifies five CB motifs within COX-1, two within COX-2 and four within COX-3; each caveolin containing a pore-lining helix C-terminal to a TM helix–turn–helix. Channel formation involves interaction between multiple pore-lining regions within protein subunits and/or dimers. PoreWalker analysis lends support to the D-channel model of proton translocation. Under physiological conditions, caveolins may introduce channel formers juxtaposed to those in COX-1, COX-2 and COX-3, which together with cholesterol may form channel(s) essential for proton translocation through the inner mitochondrial membrane.

1. Introduction

The terminal enzyme of the respiratory chain, cytochrome c oxidase (EC 1.9.3.1, CcO), consists of 13 subunits (in vertebrates) and comprises one member of the heme-copper oxygen reductases in which electron transfer is linked to movement of protons and water across the mitochondrial membrane (reviewed in [1–4]). Subunit 1 (COX-1) is the catalytic subunit of CcO. Electrons originating in cytochrome c are transferred via the copper A center of subunit 2 and heme A of subunit 1 to the bimetallic center formed by heme a3 and copper B in subunit 1, where O_2 is reduced to water. In each catalytic cycle, COX-1 receives an electron from each of four cytochrome c molecules, and transfers them to a single oxygen molecule, converting molecular oxygen to two molecules of water. In the process COX-1 obtains four protons from the inner aqueous phase to make water, while four other protons are translocated across the mitochondrial inner membrane, establishing a proton-electrochemical potential that is used by the ATP synthase to produce ATP. CcO crystallizes as a dimer, generally viewed as the functional unit within the inner mitochondrial membrane. Although both monomeric and dimeric CcO are highly active in terms of electron transfer, the dimeric form may be essential for proton translocation (reviewed in [5]).

The focus of the present work is on identification of possible proton and/or water channels within CcO in the inner mitochondrial membrane. The respiratory chain is embedded in the mitochondrial inner-membrane and consists of four large membrane protein assemblies (i.e.: NADH quinone oxidoreductase, complex I; cytochrome bc1, complex III; cytochrome c oxidase, complex IV; ATP synthase, complex V) plus additional small electron carriers (quinones and cytochrome c). Complexes I, III and IV utilize a series of electron transfers whose paths are coupled with proton translocation from the inside (mitochondrial matrix) to the intermembrane space (IMS), leading to the electrochemical proton gradient ultimately utilized by ATP synthase to transform ADP into ATP. Although oxygen can diffuse freely through the lipid membrane, and components of the electron transfer chain are known, to date, the mitochondrial pathway(s) by which proton

* Corresponding author at: Albert Einstein College of Medicine, Bronx, NY 10461, USA. Tel.: +1 212 473 9760.
E-mail address: gene.morrill@einstein.yu.edu (G.A. Morrill).

http://dx.doi.org/10.1016/j.bbamem.2014.07.011

movement is coupled to oxygen reduction remains unclear and proton and/or water channels have not been established. The inner mitochondrial membrane also contains Aquaporin-8 (Accession # P56404), a water-specific channel-former that permits water to move in the direction of an osmotic gradient [6]. Following movement into the intermembrane space, molecules up to 1.5 kDa freely diffuse through the outer mitochondrial membrane via large pores formed by VDAC, a voltage-dependent anion channel (reviewed in [6]).

Using computational analysis of the topology of the human CcO (complex IV), we find that: 1) of the 12 transmembrane (TM) helices identified in CcO subunit-1 (COX-1), 9 are pore-lining regions (possible channel formers), many containing overlapping caveolin and cholesterol binding motifs, 2) both TM helices of subunit-2 (COX-2) and 5 of the 6 TM helices in subunit-3 (COX-3) are also pore-lining regions with overlapping caveolin binding motifs, and 3) caveolin contains a pore-lining region associated with a membrane helix–turn–helix contributing an additional channel former. A single long channel containing amino acids from COX-1, COX-2 and COX-3 (plus heme a_3 and both Cu_A and Cu_B sites) can be identified from computational analysis of the crystallography data. This channel may be involved in proton movement. It is important to note that caveolins have not been identified in either CcO crystals or the CcO-containing membrane preparations used to study CcO activity. However, significant concentrations of caveolin have been shown in mitochondria [7,8] and mitochondrial function is abnormal in caveolin-knockout mice [9]. Our finding of the presence of multiple caveolin binding motifs in CcO subunits is further evidence of an important role of caveolins in mitochondrial function.

2. Materials and methods

2.1. Protein sequence sources

The amino acid sequences of human cytochrome c oxidase subunits and caveolin-1, 2 and 3 were downloaded from the ExPASy Proteonomic Server of the Swiss Institute of Bioinfomatics (http://www.expasy.org; http://www.uniprot.org). About 98% of the protein sequences provided by UniProtKB are derived from the translation of the coding sequences (CDS) which have been submitted to the public nucleic acid databases, the EMBL-Bank/Genbank/DDBJ databases (INSDC). Amino acid sequences were compared using the Pairwise Sequence Alignment software (LALIGN) at http://www.ebi.ac.uk/Tools/services/web lalign/ to find internal duplications by calculating non-intersecting local alignments [10]. The Emboss Water protocol (version 36.3.5e Nov, 2012; preload8) used here employs the Smith–Waterman algorithm (with modified enhancements) to calculate the local alignment of two sequences [10].

2.2. Secondary structure predictions

Secondary structures were predicted by PSIPRED v. 3.0; http://bioinf.cs.uci.ac.uk/psipred/ [11] and PredictProtein; (http://rostlab.org/owiki/index.php/PredictProtein) [12]. The PSIPRED secondary structure prediction method is based on position-specific scoring matrices. PredictProtein provides multiple sequence alignments and predictions of secondary structure, residue solvent accessibility, and the location of TM helices.

2.3. Transmembrane (TM) helix and pore-lining region predictions

The position of TM helices was predicted using: 1) the TOPCONS algorithm [13]; (http://topcons.cbr.su.se), 2) Phobius: (predicts TM topology and signal peptides), (http://phobius.cgb.ki.se and http://phobius.btnf.ku.dk) European Biomathematics Institute [14], 3) PredictProtein [12]: (http://ebi.ac.uk/~rost/predictprotein), 4) the MEMSAT-SVM server [15]: (http://bioinfo.cs.ucl.ac.uk/psipred/), and 5) TMHMM [16], a method based on a hidden Markov model available at: (http://www.cbs.dtu.dk/services/TMHMM/). Pore-lining regions in transmembrane protein sequences were predicted using the method of Nugent and Jones [17]: (http://bioinf.cs.ucl.ac.uk/psipred/).

2.4. TMKink: a method to predict transmembrane helix kinks

Meruelo et al. [18] have identified distinct residue preferences in kinked versus non-kinked helices and have exploited these differences and residue conservation to predict kinked helices using a neural network algorithm. The kink predictor, TMKink, is available at http://tmkinkpredictor.mbi.ucla.edu/.

2.5. PoreWalker 1.0: a method for the detection and characterization of TM protein channels from their 3D Structure

PoreWalker [19] is a stepwise procedure in which the pore center and pore axis are identified and optimized using geometric criteria, and the biggest and longest cavity through the protein is then predicted. Pore features, including diameter profiles, pore-lining residues, size, shape and regularity of the pore are calculated, providing a characterization of the longest channel in the structure. The software is available as a web-based resource at http://www.ebi.ac.uk/thornton-srv/software/PoreWalker/.

2.6. MPRAP: an accessibility predictor for α-helical transmembrane proteins

By including complete α-helical transmembrane proteins in the training of MPRAP it is possible to predict surface water accessibility accurately both inside and outside the plasma membrane [20]. This predictor can aid in the prediction of 3D structure and in the identification of erroneous protein structures. A web-server for MPRAP is available at http://mprap.cbr.su.se/.

2.7. Leucine-rich repeats (LRRs)

LRR (leucine-rich repeat) regions have been identified in viruses, bacteria, archaea and eukaryotes (reviewed in [21]). LRR motifs are involved in protein–ligand and in protein–protein interactions and each motif can be divided into a highly conserved segment (HCS) and a variable segment (VS). The HCS consists of an 11 residue sequence, LxxLxLxxNxL, or a 12 residue sequence, LxxLxLxxCxxL, in which "L" is Leu, Ile, Val or Phe, "N" is Asn, Thr, Ser or Cys, and "C" is Cys, Ser or Asn.

2.8. Caveolin-binding motifs

Using a GST-fusion protein containing the caveolin scaffolding domain as a receptor to select peptide ligands from a bacteriophage display library, Couvet et al. [22] identified at least two related but distinct caveolin binding motifs, ΦxxxxΦxxΦ and ΦxΦxxxxΦ (where Φ represents an aromatic amino acid, W, Y, or F), that have been shown to interact with caveolin in most proteins.

2.9. The CRAC domain

CRAC is a short linear amino acid motif that mediates binding to cholesterol and stands for **C**holesterol **R**ecognition/Interaction **A**mino acid **C**onsensus sequence [23]. In a C-terminus to N-terminus direction the motif consists of a branched apolar Leu (L) or Val (V) residue, followed by a segment containing 1-5 of any residues, followed by a mandatory aromatic Tyr (Y) residue, a segment containing 1-5 of any residues, and finally a basic Lys or Arg. In the one letter amino acid codes the algorithm is (L/V) − X_{1-5} − (Y) − X_{1-5} − (K/R).

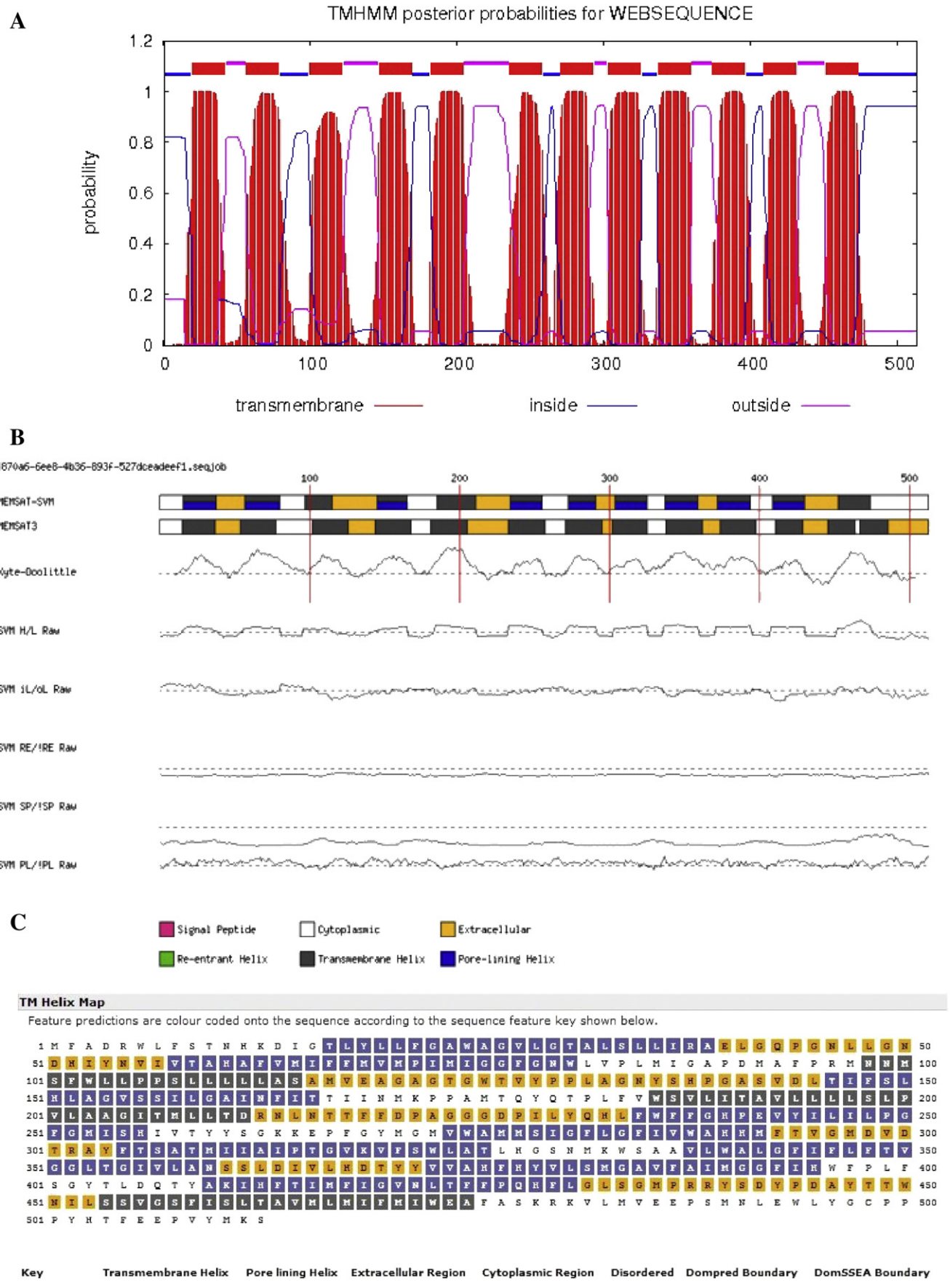
A
TMHMM posterior probabilities for WEBSEQUENCE
probability
transmembrane
inside
outside
B
8c4870a6-6ee8-4b36-893f-527dceadeef1.seqjob
MEMSAT-SVM
MEMSAT3
Kyte-Doolittle
SVM H/L Raw
SVM iL/oL Raw
SVM RE/!RE Raw
SVM SP/!SP Raw
SVM PL/!PL Raw
C
Signal Peptide
Cytoplasmic
Extracellular
Re-entrant Helix
Transmembrane Helix
Pore-lining Helix
TM Helix Map
Feature predictions are colour coded onto the sequence according to the sequence feature key shown below.
Key
Transmembrane Helix
Pore lining Helix
Extracellular Region
Cytoplasmic Region
Disordered
Dompred Boundary
DomSSEA Boundary

2.10. The CARC domain

A second cholesterol recognition domain similar to the CRAC domain (CARC) has been identified [24]. The CARC domain is comparable to the CRAC domain but exhibits the opposite orientation along the polypeptide chain ("inverted CRAC"), i.e. (K/R) − X_{1-5} − (Y/F) − X_{1-5} − (L/V). CARC is distinct from CRAC in that the central amino acid can be either Y or F.

3. Results and discussion

3.1. Transmembrane (TM) helix topology and pore-lining regions within the cytochrome c oxidase subunits

Fig. 1 compares the TM helix topology of COX-1 using a method based on the hidden Markov model [16], TMHMM (upper graphics A), the support vector machine (SVM)-based TM topology predictor MEMSAT-SVM (middle graphics B) [25] and the MEMSAT-SVM predictor of pore-lining regions (lower graphics C) [17]. Antibody and chemical labeling experiments indicate that subunits COX-1, COX-2 and COX-3, and most (but not all) of the nuclear-encoded subunits span the inner mitochondrial membrane [1,2]. The transmembrane (TM) helix has been described by Hilldebrand [26] as a membrane-spanning 17.3 ± 3.1 (SD, N = 160) amino acid sequence with a hydrogen-bonded helical configuration, including α, 3_{10} and π-helices. The α-helix is very common, while the 3_{10} helix is found at the ends of the TM α-helix. π-helices are rare. In addition to TM helices, membrane proteins may contain a cavity (or pore) which spans the membrane with an opening on each side of the plasma membrane. The "pore" often runs parallel to TM helices, forming the path along which ions travel with adjacent structures determining pore specificity (reviewed in [17]). Nugent and Jones [17] have developed a computational method capable of identifying pore-lining regions in membrane proteins from sequence data alone, which may be used to determine pore stoichiometry (number of TM helices with pore-lining regions required to form a pore). Pore-lining regions are usually enriched in negatively (e.g. E, D) or positively charged residues (e.g. K, R, H). Four features were used to train a support vector regression model: sequence length, the number of pore lining residues, with the target value set to the number of subunits contacting the pore within the membrane region.

As indicated in the upper graphic A of Fig. 1, the hidden Markov model (TMHMM) predicts 12 equally distributed TM helices (shown as red bars). The MEMSAT-SVM (support vector machine) projection (upper graphic B) also predicts 12 TM helices whereas a method based on neural networks, MEMSAT3 (lower graphic B) [15] predicts that TM-12 may be two TM helices. The MEMSAT-SVM projection indicates both the N- and C-terminal amino acids (clear sequences) are within the mitochondrial matrix whereas alternate loops (orange sequences) extend into the intermembrane space. The plots underneath the schematic topology diagram (middle, B) show the raw scores generated by the SVM's that distinguish between TM helices and loop regions (H/L), inside loops and outside loops (iL/oL), reentrant loops or non-reentrant loops (RE/!RE) and signal peptides or non-signal peptides (SP/SP!). The topology of COX-1, COX-2 and COX-3 are compared in Table 1.

The Nugent and Jones method identifying pore-lining regions [17] predicts the likelihood of a transmembrane helix being involved in pore (channel) formation and determines the number of subunits required to form a complete pore (see Methods). As shown by this method, helices 1, 2, 4, 6, 7, 8, 9, 10 and 11 of COX-1 are predicted to be pore-lining regions (graphic C). Similar analyses of COX-2 and COX-3 using MEMSAT-SVM, indicate that the COX-2 subunit contains 2 TM helices (both are pore-lining regions, Table 1), whereas the COX-3 subunit contains 6 TM helices (5 being pore-lining regions; Table 1). The COX subunits in turn form an aggregate in the inner mitochondrial membrane, and in the presence of cardiolipin, form a homodimer (reviewed in [27]). Taken *In toto*, the three subunits of the homodimeric complex contains 40 TM helices, 32 of which may be pore-lining regions (summarized in Table 1).

It should be noted that about half of all transmembrane helices contain bends and other deviations often referred to as "kinks" [28,29]. As noted by Meruelo et al. [18], distortions in helix geometry may facilitate conformational changes required for protein function by providing sites of flexibility [30,31] and can be important for positioning key residues precisely in the protein structure. Kinks that open the polar backbone to alternative hydrogen bonds often attract water molecules, thus providing a polar region within the hydrophobic core [32]. Using TMKink (see Materials and methods) to predict transmembrane helix kinks in COX-1, Table 2 indicates which of the 12 TM helices (and/or pore-lining regions) contain kinks. Residues in black indicate non-kinked regions whereas those highlighted in red correspond to correctly predicted kinks (true positives). If present, false negatives and incorrectly predicted kinks would be highlighted in green and blue, respectively. As indicated, 7 of the 12 helices (1, 2, 5, 7, 8, 9 and 11) contain kinks, whereas 3, 4, 6, 10 and 12 do not. Thus, as predicted by TMKink, only pore-lining regions 4, 6, and 10 and helices 3 and 12 represent highly ordered amino acid helical structures connecting the mitochondrial matrix and inter membrane space.

3.2. Optimal helical packing arrangements within cytochrome c oxidase subunit-1 (COX-1)

Nugent et al. [33] have developed a method to aid in determining possible 3D packing arrangements for TM helices. A support vector machine (SVM) classifier, trained using lipid exposed residue profiles labeled according to molecular dynamics simulation data [34] is used to predict per residue lipid exposure. This information is combined with PSI-BLAST profile data for each interacting residue and additional sequence-based data serves as output for an SVM to predict residue contacts. Combining these results with predicted topology data, helix–helix interactions can then be used for proteins containing up to 13 helices and to arrange the helices with a graph-based approach. In studies of a protein crystallographic database by Nugent et al. [33], in 14 of 23 cases where all helix–helix interactions were successfully predicted, the optimal helical packing arrangement closely resembled a 2D slice taken from the crystal structure of the same molecule approximately normal to the likely plane of the lipid bilayer. In 51 additional cases, 34 were partially predicted while 17 had no predicted interactions.

As shown in Fig. 2, the TM helices within *Homo sapiens* COX-1 have multiple interactions and all form a tight semicircular packing arrangement perpendicular to the membrane surface. Crystallographic analysis of *Bos taurus* CcO indicates that the COX-1 helical array is also cylindrical and oriented perpendicularly to the membrane surface [35]. An LALIGHN [10] comparison of COX-1 from *Bos taurus* (P00396) and *Homo sapiens* (P00395) indicates a 91.6% identity in a 511 amino acid overlap (1–511:1–511) with a Waterman:Eggert score of 3252. The helical packing array method of Nugent et al. [33] predicts that COX-1

Fig. 1. A comparison of the topology of cytochrome c oxidase subunit-1 (COX1 *Homo sapiens*, P00395) using the hidden Markov model [16] TMHMM (upper graphic A), the support vector machine-based TM topology predictor MEMSAT-SVM (middle graphic B) [15] and the MEMSAT-SVM predictor of pore-lining regions (lower graphic C) [17]. The plots underneath the schematic topology diagram (middle, B) show the raw scores generated by the SVM method that distinguish between TM helices and loop regions (H/L), inside loops and outside loops (iL/oL), reentrant loops or non-reentrant loops (RE/!RE) and signal peptides or non-signal peptides (SP/SP!). Transmembrane helices are indicated in red (A, upper), in black (B, middle) and as black or blue squares (C, lower). Blue squares (C) also indicate predicted pore-lining regions. Inter-membrane loops are in yellow (C, lower). The amino acid sequences are those published in the Swiss Protein Knowledgebase (www.uniprot.org). See Materials and methods for details.

Table 1
Transmembrane (TM) helix topology, pore-lining regions and motifs in the functional core subunits of cytochrome c oxidase.

Protein	Accession #	Sequence length	TM helices MEMSAT-SVM	Pore-lining regions	Caveolin-binding motifs	Leucine-rich repeats	CRAC/CARC motifs
Cytochrome c oxidase subunit 1	P00395	513 aa	12	9	5	1	5
Cytochrome c oxidase subunit 2	P00403	227 aa	3	3	2	0	1
Cytochrome c oxidase subunit 3	B0Z6N9	261 aa	6	5	4	1	2

contains 13, not 12, TM helices in both *Bos taurus* and *Homo sapiens* proteins. Consistent with this, MEMSAT3 analysis of COX-1 indicates that TM-12 may exist as two TM helices yielding a total of 13 helices (Fig. 1).

To compare crystallographic and computational analysis of helix topology, the predicted helices in *Bos taurus* COX-1 were analyzed using the two methods. Fig. 3 outlines the 514 amino acid sequence using single letter amino acid codes. Underscoring denotes the TM helices as predicted by the MEMSAT-SVM server [11]; red highlights denote the TM helical regions as determined by crystallography [35]. As can be seen there is a good correlation between crystallographic and computational methods although most of the TM helical regions predicted by the MEMSAT-SVM server were a few amino acids longer. After merging TM-12 and TM-13 and inverting the array in Fig. 2, the helical packing arrangement of individual helices using the method of Nugent et al. [33] is similar to the schematic localization of the individual TM helices of COX-1 based on the published 2.8 Å crystal end-on structure of bovine heart cytochrome c oxidase COX-1 [35]. Both *Homo sapiens* (Fig. 2) and *Bos taurus* [35] exhibited three semicircular helical arrays, each composed of four to five individual helices, that form a "whirlpool" with a quasi-threefold axis of symmetry as viewed from the top.

3.3. Caveolin and cholesterol binding motifs/domains in cytochrome c oxidase

Fig. 4 outlines a 513 amino acid sequence of *Homo sapiens* COX-1 using single letter amino acid codes. The nine pore lining-helical regions are underlined in bold, whereas the 3 non-pore-lining TM helices are double-underlined. A comparison of the helical array for Homo sapiens COX-1 in Fig. 2 and the crystallographic array published for *Bos Taurus* [35], indicates that Cu_B and heme a3 of the bimetallic center are associated with pore-lining regions (TM-6, TM-7 and TM-10) that form a helix cluster in COX-1. The axial ligands of Fe in heme A are H^{61} within the pore-lining region TM-2 and H^{378} within pore-lining region TM-10. Cu_B is associated with pore-lining regions TM-6 (H^{240} and Y^{244}) and TM-7 (H^{290} and H^{291}); whereas the axial ligand of Fe in heme a3 is associated with the pore-lining region TM-10 (H^{376}). Electrons originating in cytochrome c are transferred via the copper A center of COX-2 and heme A of COX-1 (TM-2, TM-10) to the bimetallic center formed by heme a3 (TM-10) and Cu_B (TM-6, TM-7).

Sequence analysis of COX-1 indicates the presence of several unique amino acid motifs and/or domains (Fig. 4). These include: 1) caveolin binding motifs ΦxxxxΦxxΦ and ΦxΦxxxxΦ (highlighted in red), 2) cholesterol-binding CRAC (L/V) − X_{1-5} − (Y) − X_{1-5} − (K/R) or inverse CRAC (CARC) domains (K/R) − X_{1-5} − (Y/F) − X_{1-5} − (L/V) (highlighted in blue or underlined in blue and labeled as CRAC or CARC), and 3) leucine-rich repeats (LxxLxLxxNxL, or LxxLxLxxCxxL) common to plant steroid receptors (highlighted in green) [36]. As shown in Table 1, COX-1, COX-2 and COX-3 contain 5, 2 and 4 caveolin-binding motifs, respectively. The same subunits contain 5, 1 and 2 cholesterol binding (CRAC/CARC) domains, respectively. A leucine-rich repeat (LRR) in COX-1 overlaps the C-terminus of TM-5 (^{190}ITAVLLLLSLPV^{201}). Another LRR is seen in COX-3 (Table 1). LRR's are involved in protein–ligand and in protein–protein interactions and have been largely described in plants; each motif can be divided into a highly conserved segment (HCS) and a variable segment (VS) [21]. LLRs have been implicated in steroid binding [36] and their presence may reflect steroid regulatory sites within the cytochrome c oxidase complex.

Caveolin is an unusual protein that can exist both as an integral membrane protein and a soluble protein in multiple cell compartments (reviewed in [37]). A variety of proteins have been identified that interact either with caveolin-1 or tyrosine-phosphorylated caveolin. In addition, caveolin interacts with both lipids and lipid anchors on proteins [37]. Four of the five caveolin binding (CB) motifs in COX-1 overlap the N-cap region of TM helices 5, 6, 7 and 10 (Fig. 4). A fifth CB motif is located in the C-terminal helix-free region (^{502}YHTFEEPVY^{510}). MPRAP analysis [20] identifies 74 solvent accessible residues of COX-1 and predicts that at least 431 of the total 513 amino acid residues are buried within the hydrophobic environment. Of the 74 residues designated as solvent accessible, many are associated with the CB motifs in the N-cap regions of TM-6 and TM-7 and with the N-cap regions of TM-1, TM-3, TM-8, TM-9, TM-11 and TM-12. Examination of both the X-ray crystallography cross-sections [35] and the predicted helical packing arrangement from MEMPACK (Fig. 2) indicates that two of the four helices containing CB motifs (TM-5, TM-7) are localized on the periphery of the 12-helix bundle. The two other helices (TM-6, TM-10) are associated with heme a_3 and the Cu_B sites.

In addition to five CB motifs, five putative cholesterol binding domains are present in COX-1. Cholesterol binding CRAC domains are present C-terminal to TM-6 (^{258}VTYYSGK^{264}) and overlap the N-terminal region of TM-11 (^{405}LDQTYAK^{411}). CARC (inverse CRAC) domains overlap the intracellular loop and TM-3 helix (^{96}RMNNMSFWLL^{105}), the intracellular loop between TM-6 and TM-7 (^{265}KEPFGYMGMV^{274}) and the pore-lining region within TM-8 (^{319}KVFSWL^{324}). The ^{265}K–^{274}V sequence containing the overlapped CARC and CB motifs is underlined in blue. Fantini and Barrantes suggest [38] that the variable segments (1–5) separating L/V from Y and Y from K/R in CRAC and CARC should be apolar if they are embedded in or overlap apolar regions (TM helices). The five sequences identified in COX-1 appear to qualify as cholesterol-binding domains.

A CRAC motif has been previously identified in caveolin 1 (^{94}VTKYWFRY^{101}) (reviewed in [39]). Further analysis here indicates the presence of three additional inverse CRAC motifs (^{66}KIDFEDV^{71};

Table 2
Prediction of transmembrane (TM) helix kinks in COX-1 using TMKink [18]: red residues indicate kinks.

TM-1	TM-2	TM-3	TM-4	TM-5	TM-6	TM-7	TM-8	TM-9	TM-10	TM-11	TM-12
A	V	A	T	L	F	M	F	N	Y	L	S
R	T	S	I	L	W	H	T	A	V	F	S
I	A	A	F	M	F	A	M	L	V	H	V
L	H	L	S	T	G	W	I	V	A	Q	G
L	A	L	L	I	H	V	I	I	H	P	S
S	F	L	H	G	P	I	A	G	F	F	F
L	V	S	L	A	E	F	I	T	Y	T	I
A	M	P	A	A	V	G	P	L	V	L	S
T	I	L	G	L	Y	L	T	G	L	N	L
G	F	W	V	V	I	I	G	G	S	V	T
L	M	F	S	P	L	F	V	V	M	G	A
V	V	S	I	S	I	G	K	T	G	I	V
G	P	M	L	L	L	I	V	F	A	F	F
A	I	N	G	L	P	S	F	I	I	M	A
W	G	N	A	L	G	M	S	F	M	I	I
A	F	N	I	L	I	A	W	A	G	T	M
G	I	F	N	L	L	W	L	W	F	I	I
F	G	T	F	V	I	V	A	L	I	K	W
L	F	T	T	A	L	A	T	V	H	A	E
L	G			T	P						
Y	N			I	G						
L	W			L	S						
T				S	H						

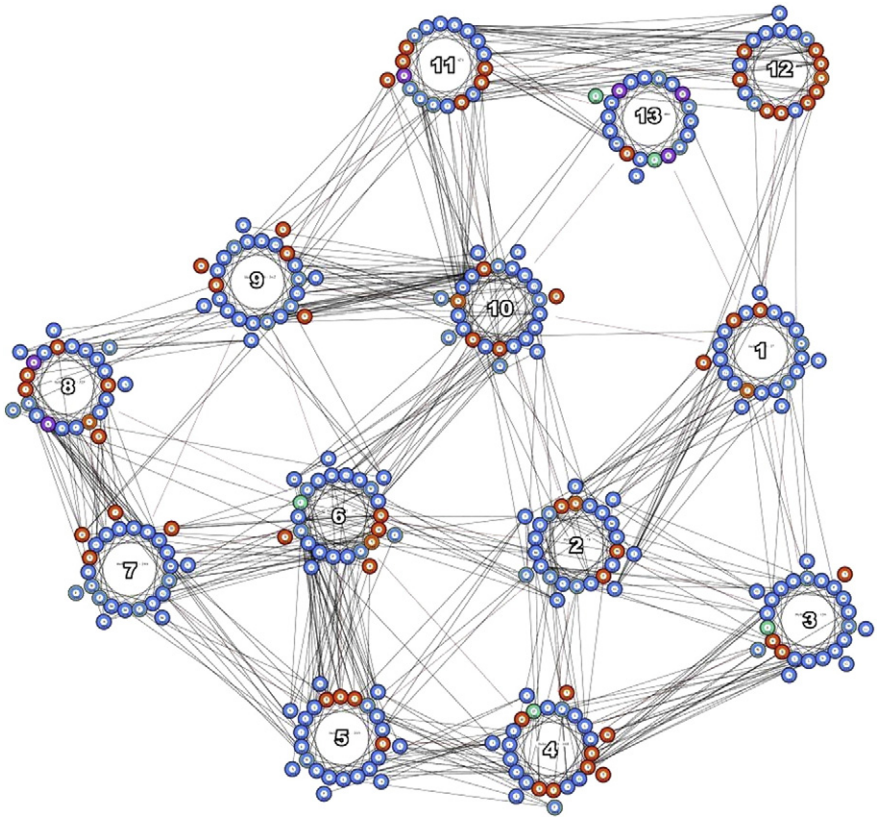

Fig. 2. Computer output for cytochrome c oxidase subunit-1 (COX1 *Homo sapiens*, P00395) showing the predicted helical packing arrangement from MEMPACK [11] (see Materials and methods). Colors in the MEMPACK cartoon indicate hydrophobic residues (blue), polar residues (red), and charged residues (green for negative, purple for positive). Lines between residues indicate a predicted interaction.

^{86}KASFTTFTV^{94}; ^{96}KYWFYRLL^{103}) in CAV-1 (Q03135). Similar analysis identifies 4 CRAC/inverse CRAC (CARC) motifs in CAV-2 (P51686) and 3 CRAC/CARC motifs in CAV-3 (P56539). This indicates that caveolins associated with CB motifs in COX-1 could, in turn, bind additional cholesterol molecules to TM-5, TM-6, TM-7 and TM-10. The cholesterol binding CARC domain (^{264}KKEPFGYMGMV^{274}) together with the overlapping CRAC domain in COX-1 and the CB motif between the two Cu_B metal ligands (in TM-6 and TM-7), could thus contribute to a cluster of bound cholesterol molecules to the protein region.

CcO is often studied using mitochondrial membrane preparations such as those prepared by the relatively rapid (3–4 h) method of Chance and co-workers [40] or the more widely used methods of Yoshikawa et al. [41] that require 3–4 days. CcO preparations are generally stored at −80 °C prior to use. Depending on the isolation procedures, CcO preparations may have become partially denatured and/or have lost functional elements such as cholesterol and caveolin. SDS-polyacrylamide gel electrophoresis of the mitochondrial preparations by Chance and coworkers [40] indicates the presence of at least 10 different polypeptide units, including a strong band in the caveolin region (22 kDa) as well as unidentified phospholipids [40]. In the description of the method of Yoshikawa et al. [41], it is stated that "a very limited analysis of protein subunit composition by NaDodSO4/ polyacrylamide gel electrophoresis supports the presence of seven major bands including subunit III". In studies of the "whole structure" of the 13-subunit oxidized cytochrome c oxidase, Tsukihara et al. [35] note that "the crystal structure reveals 13 subunits, each different from the other, five phosphatidylethanolamines, three phosphatidylglycerols and two cholates". We show here that all three mitochondrial-encoded subunits (COX-1, COX-2, and COX-3) contain multiple caveolin-binding motifs (Table 1) as well as cholesterol binding CRAC/CARC domains, indicating that caveolins and cholesterol may be complexed to the multimeric proteins under physiological conditions.

3.4. Caveolin and cholesterol transmembrane helix interactions

Caveolins are often viewed as a family of integral membrane, cholesterol-binding proteins that act as scaffolding proteins within caveolar membranes by compartmentalizing cholesterol signaling molecules [42]. Although critical for the formation of plasma membrane caveolae, as noted above, caveolins appear to have numerous functions since they are present in many locations, including mitochondria (reviewed in [7,42]). Cholesterol is concentrated both in sphingolipid-enriched membrane micro-domains such as "lipid rafts" [43,44] and in the lipid disordered phase of the plasma membrane that contains high amounts of glycerolphospholipids such as phosphatidylcholine [44]. Li et al. demonstrated [7] that caveolin-1 can be targeted to a variety of intracellular destinations, including mitochondria. More recently, Bosch et al. [8] confirmed that caveolin is not restricted to plasma membrane caveolae, and that caveolin pools are present in myriad intracellular membranes, including mitochondria, consistent with our finding of caveolin-binding motifs in CcO.

Our previous computational analysis of caveolin structure indicated that all three isoforms (CAV-1, CAV-2 and CAV-3) contain two plasma membrane spanning helices, separated by as few as 2–3 amino acid residues at the cell surface [45], not the proposed α-helical hairpin turn that does not completely traverse the membrane (e.g. [42]). As shown in Fig. 5, computational analysis using MEMSAT-SVM confirms the presence of the membrane-spanning helix–turn–helix structure in all 3 isoforms and predicts an additional pore-lining region immediately C-terminal to the membrane spanning helix–turn–helix. MEMSAT-SVM analysis indicates no interaction between the two TM helices and/or adjacent pore-lining region within caveolin.

Using TMKink [18] to predict possible transmembrane helix kinks in the three caveolin isoforms, only TM-1 contains a kink (Table 3). Residues in black indicate non-kinked regions, whereas those highlighted

in red correspond to correctly predicted kinks (true positives). As shown, TM-1 contains one or more kinks, whereas both TM-2 and the adjacent pore-lining region are kink-free. Fig. 4 further indicates that caveolin binding motifs (highlighted in red) overlap the N-terminal region of helix TM-5 as well as the pore-lining regions TM-6, TM-7, and TM-10. This indicates that caveolin binding occurs specifically at the metal binding sites in COX-1 and that the pore-lining regions may contribute to membrane channel formation.

3.5. Topology and the role of caveolin binding motifs in COX-2 and COX-3

Sequence analysis of COX-2 and COX-3 indicate that both contain binding motifs specific for caveolin, cholesterol and/or ouabain (Fig. 6). These include: 1) caveolin binding motifs ΦxxxxΦxxΦ and ΦxΦxxxxΦ (highlighted in red), 2) cholesterol-binding CRAC (L/V) — X_{1-5} —(Y) — X_{1-5} — (K/R) or inverse CRAC (CARC) domains (K/R) — X_{1-5} —(Y/F) — X_{1-5} — (L/V) (highlighted in blue or underlined in blue and labeled as CRAC or CARC), and 3) the leucine-rich repeats (LxxLxLxxNxL, or LxxLxLxxCxxL) common to plant steroid receptors [36]. COX-2 exhibits a double caveolin binding (CB) motif within TM-3 whereas COX-3 contains CB motifs within both TM-3 and TM-6. COX-3 contains a fourth CB motif in the C-terminal region. Cholesterol (CRAC and/or CARC) binding regions are present in the C-terminal region of COX-2 and overlapping both TM-2 and TM-3 in COX-3. A leucine-rich repeat (LRR) overlaps TM-2 of COX-3 (^{42}LLMLGLLTNTL^{52}).

COX-1 (Fig. 4) and COX-3 (Fig. 6) also contain caveolin binding sites associated with pore-lining regions with the potential to form membrane channels [17]. Nugent and Jones found [17] that pore-lining residue positioning within a helix typically displayed a degree of periodicity, with hydrophilic residues often separated by 3 or 4 positions, corresponding to a complete helical turn, so that a single face of the helix was oriented toward the pore or channel. This pattern was not consistent over the full length of the helix, suggesting that chains did not form a series of ideal helices packed in a tight bundle around

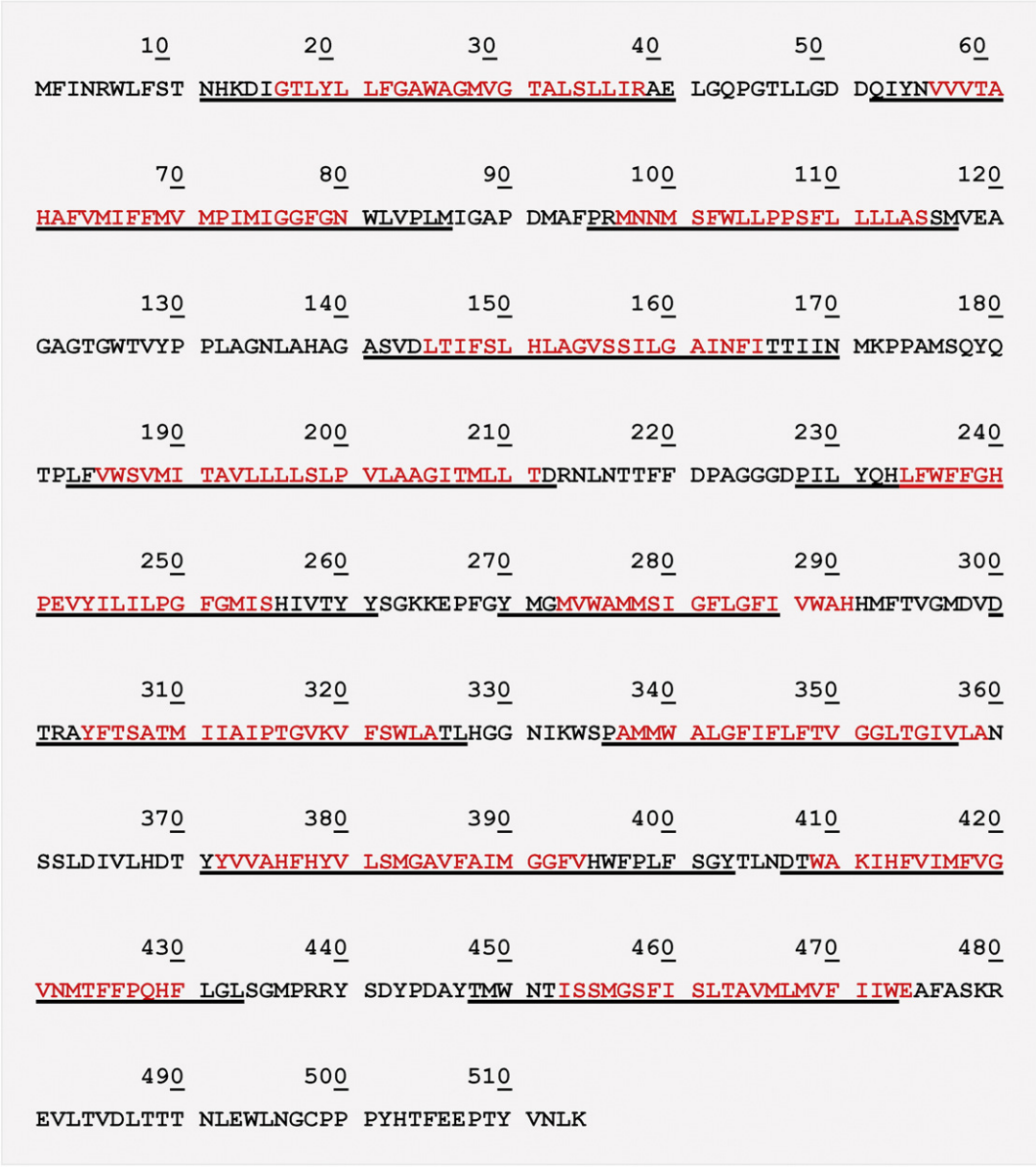

Fig. 3. Comparison of transmembrane helix regions of cytochrome c oxidase subunit-1 from *Bos Taurus* (P00396) as determined by crystallography (highlighted in red) and the MEMPACK prediction server (underlined in black). Amino acids are indicated in single letter codes. For details see text.

the pore, but that helix tilting, kinking or shielding by other helices may play a role. In the presence of caveolins, channel formation may include contributions from the pore-lining regions within the CcO–caveolin complex.

3.6. PoreWalker analysis of the functional core of cytochrome c oxidase

Typically, channel proteins contain a cavity (or pore) which spans the entire membrane with an opening on each side of the membrane. Pellegrini-Calace et al. [19] have developed an improved computational approach (PoreWalker 1.0, see Materials and methods) for the identification and characterization of channels in transmembrane proteins from their three-dimensional structure. Given a set of 3D coordinates, this method can detect and identify the pore centers and axis using geometric criteria, as well as the biggest and longest cavity through the protein. Pore features, including diameter profiles, pore-lining residues, size, shape and regularity of the pore are used to provide a quantitative and visual characterization of the channel.

Fig. 7 identifies the largest and longest channel within the complex of core subunits (COX-1, COX-2, COX-3 and COX-4) of bovine heart CcO in the fully oxidized state (2occ at 2.3Å resolution [46]) using PoreWalker. The upper image represents the pore visualization of the XY-plane section for Z < 0, the X-axis (vertical axis) being the pore axis. The middle image identifies pore-lining atoms only, and the lower image illustrates the features of the cavity in XY-planar section, for Z < 0, coordinates only. Pore-lining atoms and corresponding residues are colored in orange and blue respectively. The rest of the protein is shown in green. Red spheres indicate pore centers at 3Å steps and their size is proportional to the pore diameter at that point. PoreWalker thus identifies the largest cavity on the N-side, from which a narrow path to the opposite P side of the inner mitochondrial membrane could be detected.

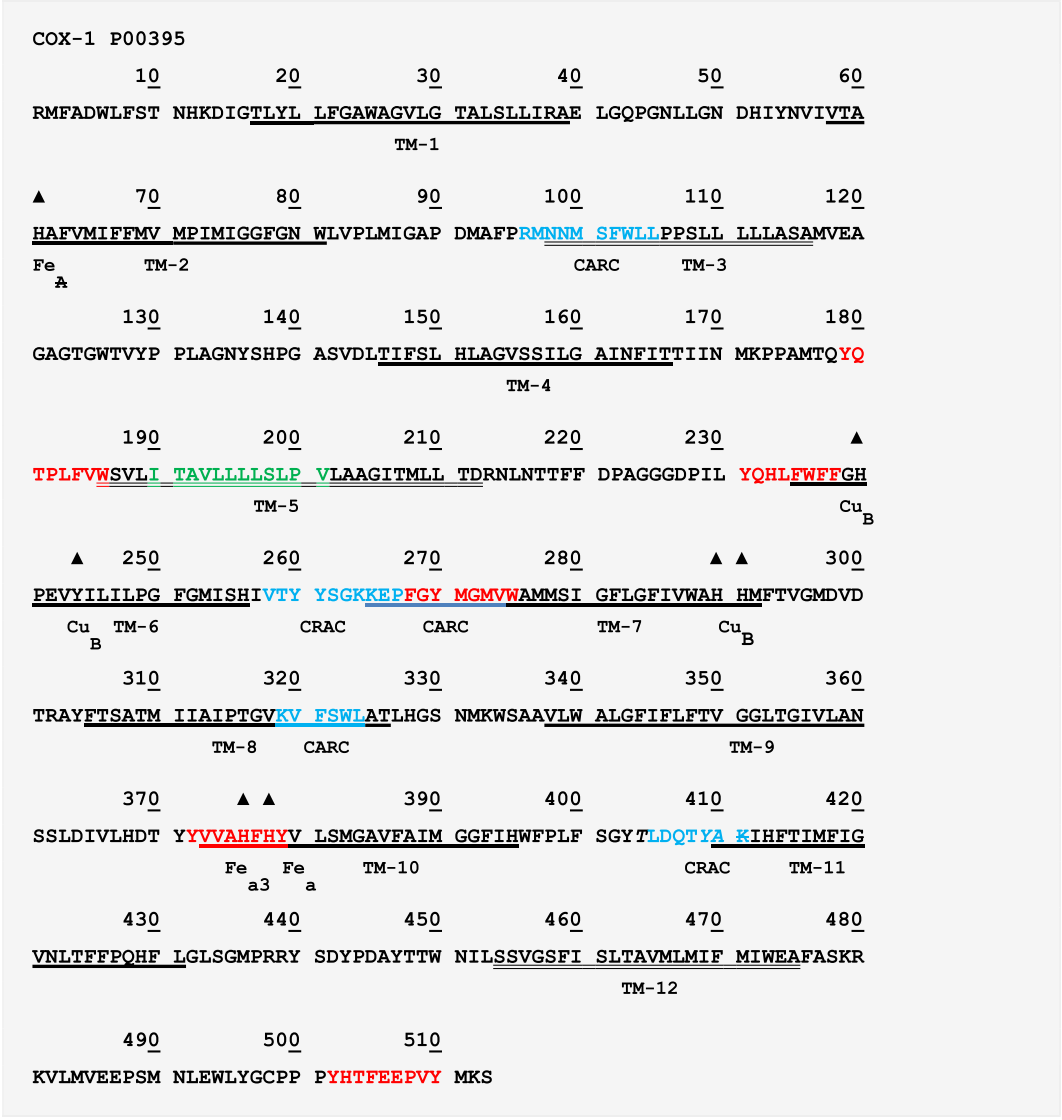

Fig. 4. Analysis of the *Homo sapiens* subunit-1 (COX-1) amino acid sequence indicates the presence of unique amino acid motifs or domains. These include: the caveolin binding motifs ΦxxxxΦxxΦ and ΦxΦxxxxΦ (highlighted in red), the cholesterol-binding CARC domain [(L/V) — X_{1-5} — (Y) — X_{1-5} — (K/R)] and CARC domain [(K/R) — X_{1-5} — (Y/F) X_{1-5} — (L/V)] (highlighted in blue), and the Leucine-Rich Repeat (LRR) common to plant steroid receptors, LxxLxLxxNxL, or LxxLxLxxCxxL (highlighted in green). Ligands of heme A, Cu_B and heme a_3 are indicated by ▲ above the amino acid and labeled underneath.

3.7. PoreWalker analysis of channel-lining amino acid residues in the functional core of cytochrome c oxidase

Channel-lining residues can be defined as amino acids contributing at least one atom to the inside surface of the pore. The channel (pore) surface can, in turn, be considered as a continuum made up of horizontal and vertical layers of atoms. In the fully oxidized functional core of 1occ [35], PoreWalker identifies 139 of the total 513 amino acids in COX-1 as channel-lining residues, with 46 of 227 residues identified as channel-lining residues in COX-2, 25 of 261 residues identified as channel-lining residues in COX-3, and 8 residues identified in COX-4. The channel-lining residues contributed by COX-1 include Cu_B associated TMs (TM-6 and TM-7) and heme a_3 associated TMs (TM-2 and TM-10) as well as TM-5 and TM-8. TM-5, TM-6 and TM-7 contain overlapping caveolin binding regions, contributing three additional pore-lining regions from bound caveolins. Contact points contributed by COX-2 include amino acid residues in the vicinity of the Cu_A center which includes two cysteines (C^{196}, C^{200}) and H^{204}. Contact points contributed by COX-3 include the external loops between TM-2 and TM-3 and between TM-5 and TM-6. Many of the COX-1 and COX-2 residues identified as pore-lining residues by PoreWalker were confirmed as accessible to water (hydrophilic sites) using the water accessibility predictor [20] for α-helical transmembrane proteins (MPRAP).

3.8. Characterization of putative water/proton channels in cytochrome c oxidase

After scrutinizing a large number of high-resolution protein atomic coordinates in the protein data bank, Miyano et al. [48] found that bound water molecules "wedge" in and stabilize large kink angles (30–40°) in transmembrane kinks so as to form an interhelical cavity. The 'wedged' water stabilizes and forms multiple hydrogen bonds to the backbone hydrogen bond acceptor(s) and/or donor(s) to cap both the helical edges as well as the side chain polar group(s) so as to neutralize the emerging charge at the bent edges caused by the helix dipole moment in the lower dielectric constant environment of the membrane spanning region [49].

The regularity of the pore cavity in CcO can be deduced from the positions of the pore centers, relative to the optimized pore axis (see [19]). Fig. 8 illustrates the predicted pore diameter profile of 2occ at 3Å steps for bovine CcO in the fully reduced state (2ocr). While the existence of a pore may seem to imply continuous connectivity, the diameter of the

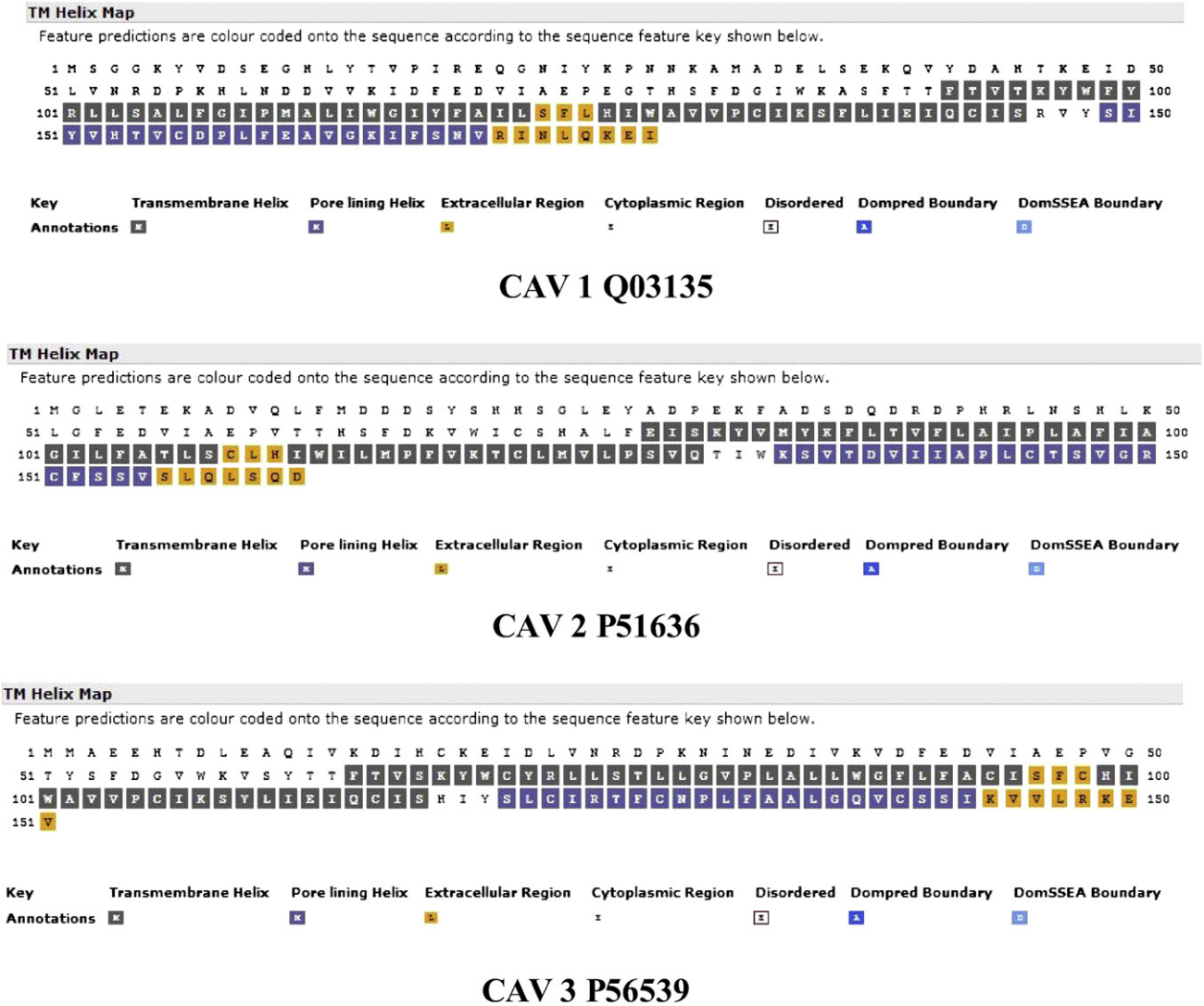

Fig. 5. Comparison of the topology of the three isoforms of *Homo sapiens* caveolin (CAV-1, top; CAV-2, middle; CAV-3, lower) using computational analysis (MEMSAT-SVM). Blue squares indicate predicted pore-lining regions. Black squares indicate transmembrane helix regions. Extracellular loops and C-terminal regions are in yellow. The amino acid sequences are those published in the Swiss Protein Knowledgebase (www.uniprot.org). See Materials and methods for details.

Table 3
Comparison of the transmembrane (TM) helical kinks in the isoforms of *Homo sapiens* caveolins using the TMKink predictor [18]: red indicates correctly predicted kinks.

CAV-1			CAV-2			CAV-3		
TM-1	TM-2	Pore	TM-1	TM-2	Pore	TM-1	TM-2	Pore
F	H	S	E	I	K	F	H	S
T	I	I	I	W	S	T	I	L
V	W	Y	S	I	V	V	W	C
T	A	V	K	L	T	S	A	I
K	V	H	Y	M	D	K	V	R
Y	V	T	V	P	V	Y	V	T
W	P	C	M	F	I	W	P	F
F	C	D	Y	V	I	C	C	C
Y	I	P	K	K	A	Y	I	N
R	K	L	F	T	P	R	K	P
L	S	F	L	C	L	L	S	L
L	F	E	T	M	C	L	Y	F
S	L	A	V	L	T	S	L	A
A	I	V	F	V	S	T	I	A
L	E	G	L	L	V	L	E	L
F	I	K	A	P	G	L	I	G
G	Q	I	I	S	C	G	Q	Q
I	C	F	P	V	F	V	C	V
P	I	S	L	Q	S	P	I	C
M	S	B	A		S	L	S	S
A		V	F		V	A		S
L			I			L		I
I			A			L		
W			G			W		
G			I			G		
I			L			F		
Y			F			L		
F			A			F		
A			T			A		
I			L			C		
L			S			I		

pore, which physically limits the size of the molecule that can flow through the channel, varies from <1 to 8 Å (See Fig. 8), and would not allow unrestricted movement of water through the channel. Alterations in the positions of specific amino acids within the putative D-channel of CcO can regulate the movement of protons/water by affecting the pore diameter at one or more locations in the channel during the redox reaction. Proton exchange with specific amino acids lining up the D-channel may directly participate in proton movement through the pore in regions of the channel where the diameter is too narrow to allow unrestricted flow of water/protons. Furthermore, a constriction in the pore may serve as a gate during the redox reaction preventing backflow of protons from the active site to the N-side of the inner mitochondrial membrane, and allowing pumping of protons to the P-side due to electrostatic repulsion of the proton by increased + ve charge on heme-iron.

A large water pocket occurs about midway through the channel and corresponds to the region containing the catalytic site formed by high-spin heme (a_3) and copper atoms (Cu_B). The channel narrow point is associated with TM-6. Since TM-6 contains a caveolin-binding motif, caveolin would contribute 3 additional helices forming a closely-packed 4-helix bundle in that region of the pore axis. Two of the four helices are pore-lining regions and a third contributed by caveolin contains a kink. The predicted topology of the pore cavity shown in Fig. 8 indicates that protons may move through the predicted channel if transient conformational changes occur at key points such as the TM-6 helical bundle during the redox-cycle. Chamberlain et al. [47] have proposed a mechanism by which salt bridge networks and hydrophobic plugs function as a gate in voltage-gated (Hv1) proton channels common to many cell types. Their molecular model indicates that electrostatic interactions are important in stabilizing both the open and closed states of Hv1 channels. In the CcO system, conformational changes could lead to amino acid bridges and/or transient increases in channel diameter. It should also be noted that the channel identified by PoreWalker in Fig. 7 represents the functional core of CcO in the crystalline form; under physiological conditions the gates may involve sequential changes in the pore-lining helices initiated by cholesterol and/'or caveolin altering the N-cap region and scaffolding domains during the redox cycle.

Crystallographic analysis of the tightly packed structure of subunit 1 (COX-1) has been variously interpreted as three possible pathways or arrays (termed K, H and D channels; see [50,51]). An important finding in our study is that all of the amino acids associated with the D (but not K or H) channel model are within the PoreWalker channel. An analysis of the residues involved in the D channel (e.g. [4,50]) indicates that the pore-lining regions TM-2, TM-3 and TM-6 plus the pore-lining region associated with the caveolin bound to TM-6 could form proton channel D. The D channel contains at least one kinked pore-lining region and, as noted above, the kinked region may be a protonated water accumulation site. Flexibility of the kinked helix may serve as a gate for movement of protonated water during the enzymatic cycle. As noted by Rich and Marechal [50], a hydrophilic array leads from the negative aqueous phase to a conserved glutamic acid (E^{242}) that is buried in COX-1 and equidistant from the two heme edges. The D channel is more extensive than the putative K channel, involving a network of 10 or more water molecules, H-bonded with N, Y and S residues, and linking D^{91} to E^{242}. E^{242} is part of a pentameric ring of amino acids (^{240}HPEVY^{244}) formed by the covalent bond between H^{240} and Y^{244}. The water cavity/channel associated with R^{38} (TM-1) is, in turn, linked by several additional waters to the peptide bond between Y^{440} and S^{441} (loop between TM-11 and TM-12), which has been suggested as a gating mechanism for the translocated proton-conduction pathway [50]. The region between residues 433 and 447 is within the putative PoreWalker channel (Fig. 7) and is consistent with the crystallographic location of CcO TM helices [35]. As seen in Fig. 2, TM-1 and TM-12 are close together and interact. TM-11 is a pore-lining region with a water containing kink, whereas TM-12 is a classical TM helix N-terminal to a caveolin binding site (^{502}YHTFEEPVY^{510}) potentially contributing one additional pore-lining region. Channels also commonly form between pore-lining regions of homotrimeric and homotetrameric structures [17]. Using FTIR spectroscopy, Marechal and Rich found [52] that weakly H-bonded water molecules within the bovine CcO structure undergo structural perturbations in response to ligand (CO) changes in binuclear center as well as to redox changes of the redox cofactor(s). They conclude that such structured water changes, working in concert with alterations of protonatable amino acids in one or more of the putative H, D and K channels, may be critical to the CcO proton/electron coupling mechanism. The making and breaking of H bonds in water chains would provide a mechanism for formation of transient proton pathways and controlled gating during catalysis. Furthermore, side-chains of hydrophobic amino acids (e.g. F) can constrict pore access from the N- or P-side of the inner mitochondrial membrane, requiring conformational change for transient pore opening as reported in the case of ammonia transporter (cit. [28]).

Since CcO exists in the mitochondrial membrane as a homodimer, channels may form between pore-lining regions generated by adjacent monomers. This is consistent with the finding that cardiolipin is essential for dimerization [27] and that four of the cardiolipin binding sites are associated with the entrance to D and H proton channels [27]. This suggests that pore-lining regions associated with both transmembrane helices and caveolins are essential for net proton movement. Studies using Raman spectra to monitor proton movement (e.g. [51]) postulate that the putative H-channel proton translocation occurs via exchangeable protons residing on the carboxyl groups of the propionates and/or the amino acid/water molecules that form H-bonds with them. The water/proton channel detected in the PoreWalker analysis passing through the bimetallic centers is consistent with rapid exchangeability of heme a_3 protons observed in Resonance-Raman studies [51]. However, the H/D exchange observed in the equilibrium states in the Raman studies is a passive entropy-driven process, which involves spontaneous

migration of protons; the H channel may contribute to this equilibrium proton exchange but might not account for active translocation of protons.

4. Conclusions

Mitochondrial DNA is the source for three critical protein subunits central to cytochrome c oxidase activity. Subunit-1 (COX-1) of cytochrome c oxidase consists of twelve tightly packed TM helices with minimal external structure and is localized to the inner mitochondrial membrane. As shown here, computational analysis of COX-1 topography indicates that 9 of the 12 TM helices are pore-lining regions (only TM-3, TM-5 and TM-12 are classical TM helices) and that multiple helix–helix interactions occur within the helical packing array similar to those seen with crystallography (Fig. 2). COX-1 contains cholesterol binding (CRAC/CARC) domains overlapping TM-3, TM-6, TM-7, TM-8 and TM-11 and a Leucine-Rich Repeat (ouabain-like steroid binding site [21]) overlapping TM-5. COX-2, on the other hand, contains only 3 TM helices (all pore-lining regions), two overlapping CB motifs, no helix–helix interactions and one cholesterol binding motif in the

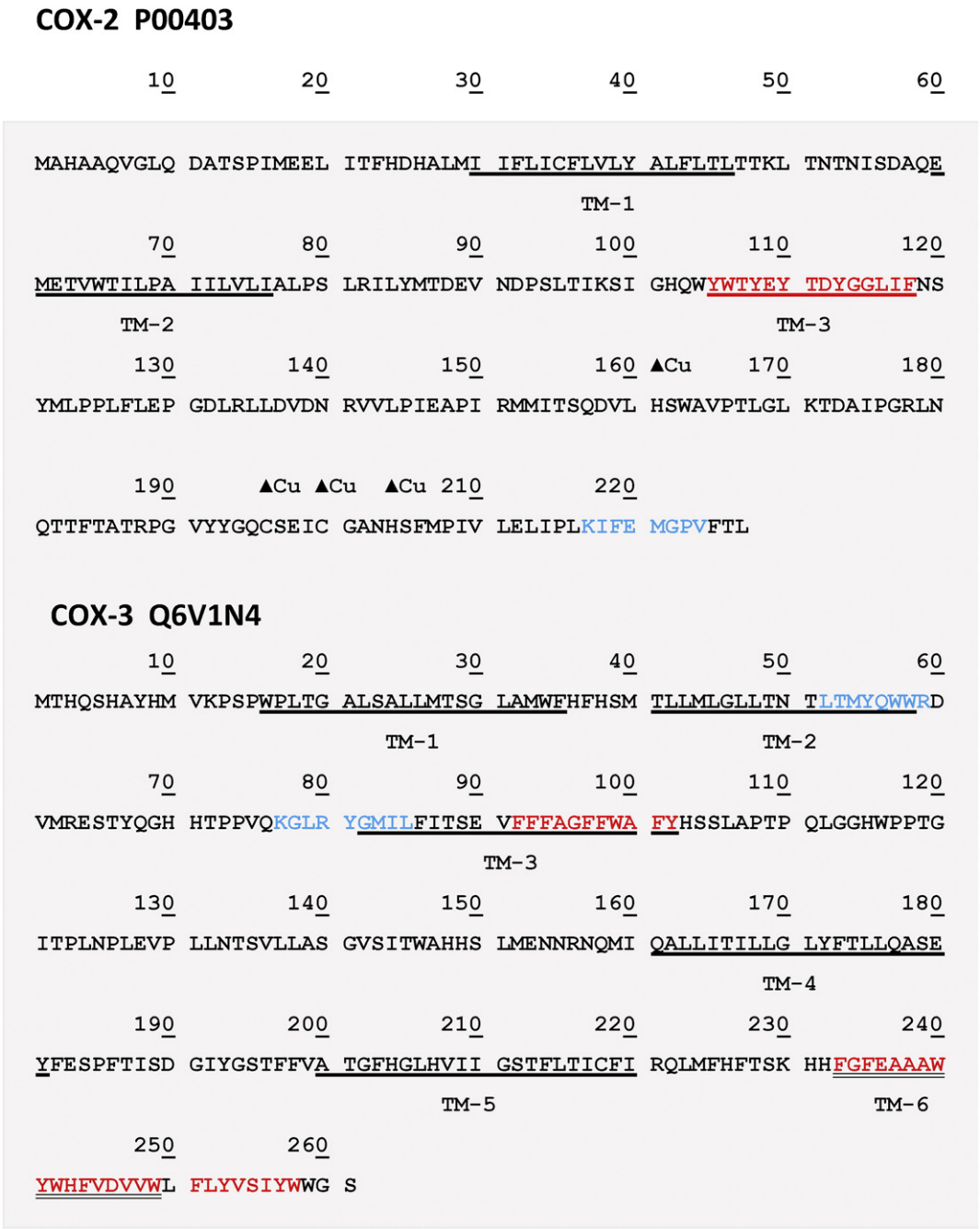

Fig. 6. Analysis of the *Homo sapiens* COX-2 (upper) and COX-3 (lower) amino acid sequences for the presence of specific amino acid motifs and/or domains. These include: the caveolin binding motifs ΦxxxxΦxxΦ and, ΦxΦxxxxΦ (highlighted in red), the cholesterol-binding CRAC (L/V) — X_{1-5} — (Y) — X_{1-5} — (K/R) or CARC (K/R) — X_{1-5} — (Y/F) X_{1-5} — (L/V) (highlighted in blue), and the Leucine-Rich Repeat (LRR) common to plant steroid receptors, LxxLxLxxNxL, or LxxLxLxxCxxL (^{42}L-^{52}L in COX-3). The transmembrane helices are underlined; the pore-lining regions are underlined with a single bold line. The ligands of Cu_A are indicated by ▲Cu. For details see Materials and methods.

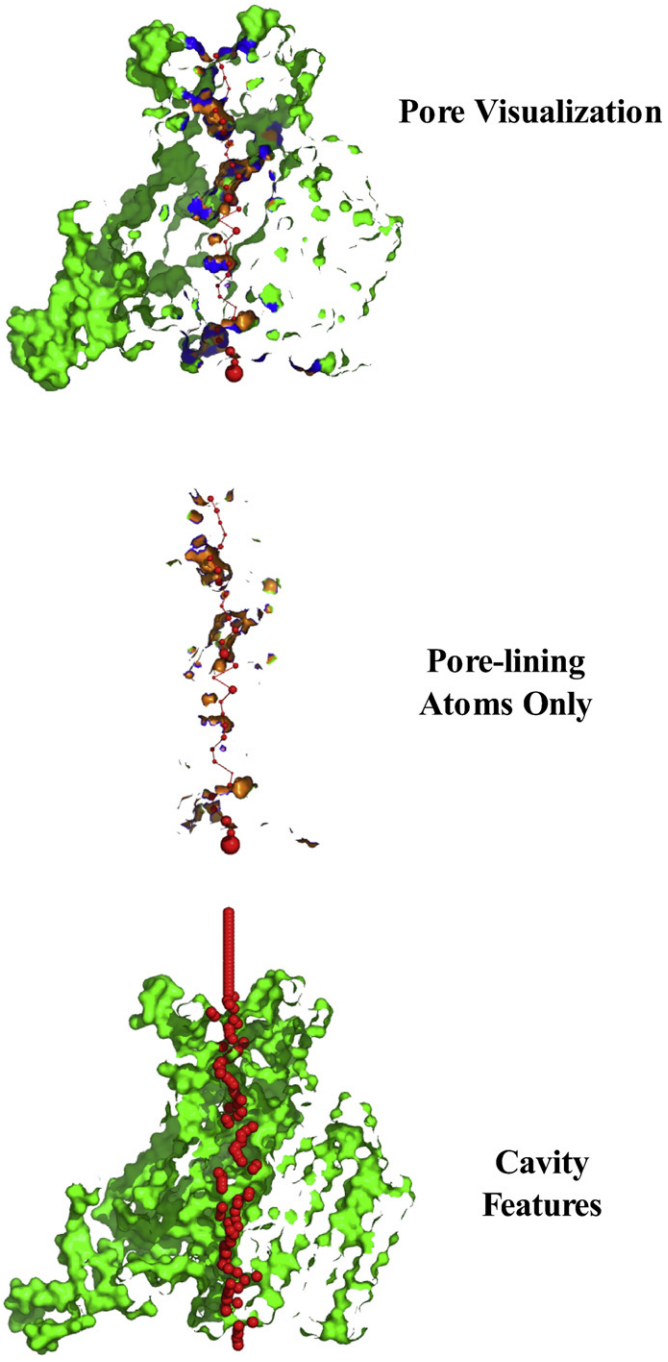

Fig. 7. A PoreWalker visual representation of the pore in the four subunit core of bovine heart cytochrome c oxidase (composite of COX-1, COX-2, COX-3 and COX-4) in the fully oxidized state (2occ, EMBL-EBI website) using the program PoreWalker 1.0 (see Materials and methods). The protein structure is colored in green and the red spheres represent pore centers at various pore heights and their diameters are proportional to the pore diameters calculated at that point. Pore lining atoms and residues are in orange and blue, respectively. Sections were obtained by cutting the protein structure along the XY plane. The top image illustrates the pore visualization, XY-plane section, Z < 0 coordinates only. The middle image illustrates the pore-lining atoms only, and the lower image visualizes the cavity features in the same plane. For details see Materials and methods.

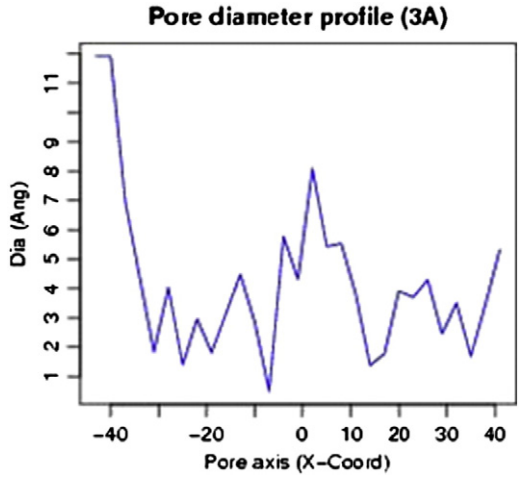

Fig. 8. PoreWalker output for the pore diameter profile in 3Å steps for the pore in the four subunit core of bovine heart cytochrome c oxidase in the fully reduced state (2ocr, EMBL-EBI website) using the program PoreWalker 1.0 (see Materials and methods). Pore axis (X-Coord): the position along the pore axis is shown as the x-coordinate in Å. Dia (Ang): pore diameter value in Å.

C-terminal region. The third subunit (COX-3) contains 6 TM-helices (5 are pore-lining regions) with extensive helix–helix interactions, four caveolin binding motifs and cholesterol binding domains overlapping TM-2 and TM-3. Like COX-1, COX-3 contains a Leucine-Rich repeat, indicative of an ouabain-like steroid binding site.

Sequence analysis indicates that four of the 12 TM helices (TM-5, TM-6, TM-7, and TM-10) of COX-1 and two of six TM transmembrane helices (TM-3 and TM-6) of COX-3 contain caveolin-binding (CB) motifs. Our finding that caveolins also contain one pore-lining region in close proximity to the existing helix–turn–helix structure [45] suggests additional sites of helix–helix interactions within both COX-1 and COX-3 under physiological conditions. Analysis of the crystallographic coordinates of the functional core (COX-1 to COX-4) using the PoreWalker program [19], predicts a transmembrane water-containing channel that encompasses the Cu_A and Cu_B centers as well as heme a_3. PoreWalker analysis also lends support to the D-channel model of proton translocation, since the PoreWalker channel contains all the essential amino acids involved in the D channel, but not the putative K or H channels. PoreWalker and Kink analysis indicate that protons move largely via water-filled caverns with likely participation from exchangeable protons of amino acid residues (Fig. 8).

As noted above, osmotic water movement across the inner mitochondrial membrane cannot be accounted for by the PoreWalker channel described in Fig. 8. Earlier studies by Calamita et al. [6] reported aquaporin 8 to be present in the inner mitochondrial membrane and suggested that aquaporin 8 played a major role in osmotic water movement between mitochondria and cytoplasm. These authors now conclude [53] that: 1) the mitochondrion is highly permeable to water, 2) the water permeabilities of inner and outer mitochondrial membrane are comparable, and 3) in spite of their high surface-to-volume ratio, mitochondria "possess facilitated pathways for water diffusion other than the AQP8 water channels". Thus, the role of channels, including those contributed by aquaporins, in mitochondrial water movement is not apparent.

The existence of cholesterol-rich regions, cardiolipin binding sites [27], and the presence of a 28–34 mol/mol molecular ratio of phospholipids/enzyme within functional CcO preparations [41], suggests that complex lipid–protein interactions occur within the mitochondrial inner bilayer under physiological conditions. As described by Chun et al. [54], changes in cholesterol content may directly affect lipid-channel protein interactions, change channel gating kinetics and participate in targeting channels to specific membrane micro-domains. A variety of integral membrane proteins, including ion channels, are sensitive to cholesterol changes in the surrounding lipid bilayer [55,56].

The heme a_3 and the Cu_B sites are within the kink-free pore-lining regions of TM-6, TM-7 and TM-10. Our finding that caveolin also contains a pore-lining region immediately C-terminal to the previously reported helix–turn–helix [45] as well as four cholesterol binding (CRAC/CARC) sites suggests that caveolin binding motifs overlapping TM-5, TM-6, TM-7 and TM-10 (Table 3) could contribute additional channel forming elements. As proposed by Nugent and Jones [17], channel formation requires contributions from multiple pore-lining regions either within a protein subunit or between subunits. The channel identified by the program PoreWalker represents contributions from several pore-lining regions in COX-1 and may be the backbone of the proton/water conducting channel. Crystallography [35], helical array patterns (Fig. 2) and PoreWalker analyses of bovine CcO (Fig. 7) indicate that the pore-lining regions within TM-5, TM-6, and TM-7 of COX-1 and TM-3 of COX-3 (as well as pore-lining regions of bound caveolins) are in close contact within the helical bundle array and localized to the surface of both subunits (Fig. 2). Although both monomeric and dimeric forms of CcO are highly active in terms of electron transfer, the dimeric form (reviewed in [5]) may be essential for proton translocation via the putative D channel and (as predicted by PoreWalker) may involve interaction with pore-lining regions of adjacent CcO subunits.

Acknowledgements

This research was supported in part by National Institutes of Health Research Grants GM-57421, HD-10463 and GM-071324.

References

[1] E. Wallin, T. Tsukihara, S. Yoshikawa, G. Von Heijne, A. Elofsson, Architecture of helix bundle membrane proteins: an analysis of cytochrome c oxidase from bovine mitochondria, Protein Sci. 6 (1997) 808–815.
[2] O.-M.H. Richter, B. Ludwig, Cytochrome c oxidase — structure, function, and physiology of a redox-driven molecular machine, Rev. Physiol. Biochem. Pharmacol. 147 (2003) 47–74.
[3] S. Yoshikawa, K. Muramoto, K. Shinzawa-Itoh, Proton-pumping mechanism in cytochrome c oxidase, Annu. Rev. Biophys. 40 (2011) 205–223.
[4] D.M. Popovic, Current advances in research of cytochrome c oxidase, Amino Acids 45 (2013) 1073–1087.
[5] J. Stanicova, E. Sedlak, A. Musatov, N.C. Robinson, Differential stability of dimeric and monomeric cytochrome c oxidase exposed to elevated hydrostatic pressure, Biochemistry 46 (2007) 7146–7152.
[6] G. Calamita, D. Ferri, P. Gena, G.E. Liquori, A. Cavalier, D. Thomas, M. Svelto, The inner mitochondrial membrane has aquaporin-8 water channels and is highly permeable to water, J. Biol. Chem. 280 (2005) 17149–17153.
[7] W.P. Li, P. Liu, B.K. Pilcher, R.G. Anderson, Cell-specific targeting of caveolin-1 to caveolae, secretory vesicles, cytoplasm or mitochondria, J. Cell Sci. 114 (2001) 1397–1408.
[8] M. Bosch, M. Mari, S.P. Gross, J.C. Fernandez-Checa, A. Pol, Mitochondrial cholesterol: a connection between caveolin, metabolism and disease, Traffic 12 (2011) 1483–1489.
[9] H.N. Fridolfsson, Y. Kawaraguchi, S.S. Ali, M. Panneerselvam, Mitochondrial-localized caveolin in adaption to cellular stress and injury, FASEB J. 26 (2012) 4637–4649.
[10] X. Huang, W. Miller, A time-efficient, linear space local similarity algorithm, Adv. Appl. Math. 12 (1991) 337–357.
[11] L.J. McGuffin, K. Bryson, D.T. Jones, The PSIPRED protein structure prediction server, Bioinformatics 16 (2000) 404–405.
[12] B. Rost, G. Yachdav, J. Liu, The predictProtein server, Nucleic Acids Res. 32 (2004) W321–W326.
[13] A. Bernsel, H. Viklund, Hennerdal, A. Elofsson, TOPCONS: consensus prediction of membrane protein topology, Nucleic Acids Res. 37 (2009) W465–W468.
[14] L. Kall, A. Krogh, E.L.L. Sonnhammer, A combined transmembrane topology and signal peptide prediction method, J. Mol. Biol. 338 (2004) 1027–1036.
[15] T. Nugent, D.T. Jones, Transmembrane protein topology prediction in support vector machines, BMC Bioinformatics 19 (2009) 874–881.
[16] A. Krogh, B. Larsson, G. von Heijne, E.L.L. Sonnhammer, Predicting transmembrane protein topology with a Hidden Markov Model: application to complete genomes, J. Mol. Biol. 305 (2001) 567–580.
[17] T. Nugent, D.T. Jones, Detecting pore-lining regions in transmembrane protein sequences, BMC Bioinformatics 13 (2012) 169–178.
[18] A.D. Meruelo, I. Samish, J.U. Bowie, TMKink: a method to predict transmembrane helix kinks, Protein Sci. 20 (2011) 1256–1264.
[19] M. Pellegrini-Calace, T. Malwald, J.M. Thornton, PoreWalker: a novel tool for the identification and characterization of channels in transmembrane proteins from their three-dimensional structure, PLoS Comput. Biol. 5 (2009) 1–16.
[20] K. Illergard, S. Callegari, A. Elofsson, MPRAP: an accessibility predictor for a-helical transmembrane proteins that performs well inside and outside the membrane, BMC Bioinformatics 11 (2010) 333–344.
[21] N. Matsushima, N. Tachi, Y. Kuroki, P. Enkhbayer, M. Osaki, M. Kamiya, R.H. Kretsinger, Structural analysis of leucine-rich repeat variants in proteins associated with human diseases, Cell. Mol. Life Sci. 62 (2005) 2771–2791.
[22] J. Couvet, M. Sargiacomo, M.P. Lisanti, Interaction of a receptor tyrosine kinase, EGF-R, with caveolins, J. Biol. Chem. 272 (1997) 30429–30438.
[23] H. Li, V. Papadopoulos, Peripheral-type benzodiazepine receptor function in cholesterol transport. Identification of a putative cholesterol recognition/interaction amino acid sequence and consenous pattern, Endocrinology 139 (1998) 4991–4997.
[24] C.J. Baier, J. Fantini, F.J. Barrantes, Disclosure of cholesterol recognition motifs in transmembrane domains of human nicoticin acetylcholine receptor, Sci. Rep. 1, 2011, 69, http://dx.doi.org/10.1038/srep00069.
[25] T. Nugent, D.T. Jones, Transmembrane protein topology prediction using support vector machines, BMC Bioinformatics 10 (2009) 159–170.
[26] P.W. Hilldebrand, S. Lorenzen, A. Goede, R. Preissner, Analysis and prediction of helix–helix interactions in membrane channels and transporters, Proteins 64 (2006) 253–262.
[27] C. Arnarez, S.J. Marrink, X. Periole, Identification of cardiolipin binding sites on cytochrome c oxidase at the entrance of proton channels, Sci. Rep. 3 (2013) 1263, http://dx.doi.org/10.1038/srep01263.
[28] S.E. Hall, K. Roberts, N. Vaidehi, Position of helical kinks in membrane protein crystal structures and the accuracy of computational prediction, J. Mol. Graph. Model. 27 (2009) 944–950.
[29] D.N. Langelaan, M. Wieczorek, C. Biouin, J.K. Rainey, Improved helix and kink characterization in membrane proteins allows evaluation of kink sequence predictors, J. Chem. Inf. Model. 50 (2010) 2213–2220.
[30] J.N. Bright, I.H. Shrivastava, F.S. Cordes, M.S.P. Sansom, Conformational dynamics of helix S6 from Shaker potassium channel simulation studies, Biopolymers 64 (2002) 303–313.
[31] L. Shi, G. Liapakia, R. Xu, F. Guarnieri, J.A. Ballesteros, J.A. Javich, Beta 2 adrenergic receptor activation. Modulation of the proline kink in transmembrane 6 by a rotamer toggle switch, J. Biol. Chem. 277 (2002) 40989–40996.
[32] P. Barth, B. Wallner, D. Baker, Prediction of membrane protein structures with complex topologies using limited constraints, Proc. Natl. Acad. Sci. U. S. A. 106 (2009) 1409–1414.
[33] T. Nugent, S. Ward, D.T. Jones, The MEMPACK alpha-helical transmembrane protein structure prediction server, Bioinformatics 27 (2011) 1438–1439.
[34] M.S. Sansom, K.A. Scott, P.J. Bond, Coarse-grained simulation: a high-throughput computational approach to membrane proteins, Biochem. Soc. Trans. 36 (2008) 27–32.
[35] T. Tsukihara, H. Aoyama, E. Yamashita, T. Tomizaki, H. Yamaguchi, K. Shinzawa-Itoh, R. Nakashima, R. Yaono, S. Yoshikawa, The whole structure of the 13-subunit oxidized cytochrome c oxidase at 2.8 Å, Science 272 (1996) 1136–1144.
[36] J. Dolan, K. Walshe, S. Alsbury, K. Hokamp, S. O'Keeffe, T. Okafuji, S.F. Miller, G. Tear, K.J. Mitchell, The extracellular leucine-rich repeat superfamily; a comparative survey and analysis of evolutionary relationships and expression patterns, BMC Genomics 8 (2007) 320–344.
[37] P. Liu, M. Rudick, R.G.W. Anderson, Multiple functions of caveolin-1, J. Biol. Chem. 277 (2002) 41295–41298.
[38] J. Fantini, F.J. Barrantes, How cholesterol interacts with membrane proteins: an exploration of cholesterol-binding sites including CRAC, CARC, and tilted domains, Front. Physiol. 4 (2013) 1–9.
[39] E.M. Epand, B.G. Sayer, R.F. Epand, Caveolin scaffolding region and cholesterol-rich domains in membranes, J. Mol. Biol. 345 (2005) 339–350.
[40] Y. Li, A. Naqui, T.G. Frey, B. Chance, A new procedure for the purification of monodisperse highly active cytochrome c oxidase from bovine heart, Biochem. J. 242 (1987) 417–423.
[41] S. Yoshikawa, T. Tera, Y. Takahashi, T. Tsukihara, W.S. Caughey, Crystalline cytochrome c oxidase of bovine heart mitochondrial membrane: composition and x-ray diffraction studies, Proc. Natl. Acad. Sci. U. S. A. 85 (1988) 1354–1358.
[42] A. Schlegel, M.P. Lisanti, A molecular dissection of caveolin-1 membrane attachment and oligomerization. Two separate regions of the caveolin-1 C-terminal domain mediate membrane binding and oligomer/oligomer interactions in vivo, J. Biol. Chem. 275 (2000) 21605–21617.
[43] R.G. Anderson, K. Jacobson, A role for lipid shell in targeting proteins to caveolae, rafts, and other lipid domains, Science 296 (2002) 1821–1825.
[44] J. Fantini, N. Garmy, R. Mahfoud, N. Yahi, Lipid rafts: structure, function and role in HIV, Alzheimer's and prion diseases, Expert Rev. Mol. Med. 4 (2002) 1–22.
[45] G.A. Morrill, A.B. Kostellow, A. Askari, Caveolin-Na/K-ATPase interactions: role of transmembrane topology in non-genomic signal transduction, Steroids 77 (2012) 1160–1168.
[46] S. Yoshikawa, K. Shinzawa-Itoh, R. Nakashima, R. Yaono, E. Yamashita, N. Inoue, M. Yao, M.J. Fei, C.P. Libeu, T. Mizushima, H. Yamaguchi, T. Tomizaki, T. Tsukihara, Redox-coupled crystal structural changes in bovine heart cytochrome c oxidase, Science 280 (1998) 1723–1729.
[47] A. Chamberlin, F. Qui, S. Rebolledo, Y. Wang, S.Y. Noskov, H.P. Larsson, Hydrophobic plug functions as a gate in voltage-gated proton channels, Proc. Natl. Acad. Sci. U. S. A. 111 (2013) E273–E282.
[48] M. Miyano, A. Hideo, H. Saino, T. Hori, K. Ida, Internally bridging water molecule in transmembrane α-helical link, Curr. Opin. Struct. Biol. 20 (2010) 456–463.
[49] L. Serrano, A.R. Fersch, Capping and α-helix stability, Nature 342 (1989) 296–299.

[50] P.R. Rich, A. Marechal, Functions of the hydrophilic channels in protomotive cytochrome c oxidase, J. R. Soc. Interface 10 (2013) 20130183.
[51] T. Egawa, S.-R. Yeh, D.L. Rousseau, Redox-controlled proton gating in bovine cytochrome c oxidase, PLoS One 8 (2013) e63669.
[52] A. Marechal, P.R. Rich, Water molecule reorganization in cytochrome c oxidase revealed by FTIR spectroscopy, Proc. Natl. Acad. Sci. U. S. A. 108 (2011) 8634–8638.
[53] G. Calamita, P. Gena, D. Meleleo, D. Ferri, M. Svelto, Water permeability of rat liver mitochondria: a biophysical study, Biochim. Biophys. Acta 1758 (2006) 1018–1024.
[54] Y.S. Chun, S. Shin, Y. Kim, H. Cho, M.K. Park, T.-W. Kim, S.V. Voronov, G. Di Palo, B.-C. Suh, S. Shung, Cholesterol modulates ion channels via down-regulation of phosphatidyl 4,5-bisphosphate, J. Neurochem. 112 (2010) 1286–1294.
[55] P.L. Yeagle, Modulation of membrane function by cholesterol, Biochimie 73 (1991) 1303–1310.
[56] O.G. Mouritsen, K. Jorgensen, Dynamical order and disorder in lipid bilayers, Chem. Phys. Lipids 73 (1994) 3–25.